

Synthesis, Characterization, and Bonding Properties of Polymeric Fullerides $AC_{70} \cdot nNH_3$ (A = Ca, Sr, Ba, Eu, Yb)

Ulrich Wedig, Holger Brumm, and Martin Jansen*^[a]

Abstract: Reduction of C_{70} with alkaline earth and rare earth metals dissolved in liquid ammonia results in metal fulleride solvates $AC_{70} \cdot nNH_3$ (A = Ca, Sr, Ba, Eu, Yb) containing linear polymeric, anionic chains ${}^{\infty}[C_{70}^{2-}]$. The compounds were characterised by means of Raman spectroscopy and single-crystal structure determination. The accurate crystal structure of $[Sr(NH_3)_8]C_{70} \cdot 3NH_3$, determined with atomic resolution, allowed for a comparison with results of quantum chemical calculations. The nature of the C–C bonds in the fulleride is analysed in detail leading to a model explaining the unexpected polymerisation of C_{70}^{2-} .

Keywords: ab initio calculations · C_{70} · polymeric fullerides · Raman spectroscopy · structure elucidation

Introduction

After the discovery of the first polymeric fullerene phases AC_{60} (A = alkali metal)^[1] a large number of compounds with covalently linked fullerenes has been synthesised especially by photochemical^[2] and pressure-induced reactions.^[3] In particular the latter route has proved to be successful; however, the connectivities achieved depend very much on the reaction conditions. Due to their low tendency to crystallise, the structures of these compounds have not been determined accurately, up to now. Only for the dimers of C_{60} (C_{120})^[4] and C_{70} (C_{140}),^[5] as well as for one polymeric C_{70} modification^[6] have satisfactory characterisations been reported. In these last two examples the cages are linked by cyclobutane-like C_4 rings, which are usually formed through a [2+2] cycloaddition across parallel double bonds of individual fullerene molecules.

Cages linked by one single bond are present in the dimeric $(C_{60})_2^{2-}$ ion^[7] and $(C_{59}N)_2$ ^[8] as well as in the polymeric high-pressure phases of Na_2RbC_{60} ^[9] and Li_3CsC_{60} .^[10] Linking in two dimensions through four single bonds is realised in Na_4C_{60} .^[11] In an earlier paper we reported on the synthesis and characterisation of a linear polymeric ${}^{\infty}[C_{70}^{2-}]$ ion in $[Ba(NH_3)_9]C_{70} \cdot 7NH_3$ (**1**).^[12]

A detailed chemical interpretation of the large variety of experimental results obtained to date is restricted by the lack of reliable structural information. Until now a complete determination of the structures, based on the refinement of all

atomic positions without applying any geometrical constraints has not been possible for any of the dimeric or polymeric fulleride species. Thus the information available does not offer a reliable basis for a detailed analysis of the structural changes to the fullerene cages due to reduction and polymerisation.

In continuation of our work on reducing fullerenes with alkaline earth or rare earth metals in liquid ammonia forming compounds that contain linear polymeric ${}^{\infty}[C_{70}^{2-}]$ chains, we were able to synthesise $[Sr(NH_3)_8]C_{70} \cdot 3NH_3$ (**2**). We have analysed **2** by means of single-crystal X-ray structure analysis, Raman spectroscopy and quantum chemical methods. As can be seen from the Raman spectra, the related compounds containing Ca, Eu and Yb also contain the linear fulleride chains. The exact crystal structure analysis of **2** allows for the comparison with theoretical investigations, both to test the reliability of ab-initio methods to predict details of the structure of fullerides and to analyse the local properties of the various C–C bonds in the C_{70} cage. C_{70} can be described as being built up from two caps that are comparable to one half of C_{60} which are connected by a phenylene-type belt.^[13] In the following discussion we refer to these structural elements when we point to specific sites in the cage.

Results and Discussion

Structure: The fulleride cages in **2** are linked by C–C single bonds between carbon atoms located in each of the two opposing five-membered rings along the fivefold axis of the neutral, undistorted C_{70} cage forming linear polymeric chains ${}^{\infty}[C_{70}^{2-}]$ (Figure 1). The length of the bridging bond is 1.575(3) Å, indicating sp^3 hybridization of the bridging atoms.

[a] Prof. Dr. M. Jansen, Dr. U. Wedig, Dipl.-Chem. H. Brumm
Max-Planck-Institut für Festkörperforschung
Heisenbergstrasse 1, 70569 Stuttgart (Germany)
Fax: (+49) 711-689-1502
E-mail: m.jansen@fkf.mpg.de

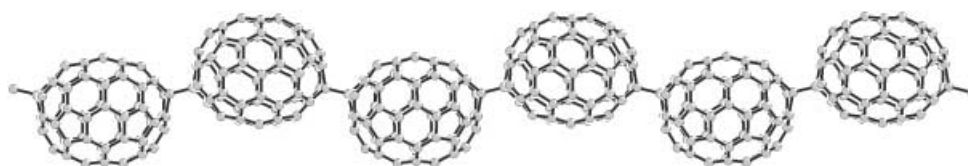


Figure 1. Molecular structure of the polymeric ${}_{\infty}[\text{C}_{70}^{2-}]$ ion. The bond length of each of the bridging C–C single bonds is 1.575(3) Å. The smallest intermolecular distance between the centres of mass of two fullerenes is 10.493 Å.

Due to the one-dimensional linkage the point group symmetry of the C_{70} unit is lowered from D_{5h} for the uncharged fullerene to C_2 (positional symmetry: C_1 ; Figure 2). Within the limits of error, the variation of bond lengths does not break this point group symmetry (Figure 3a).

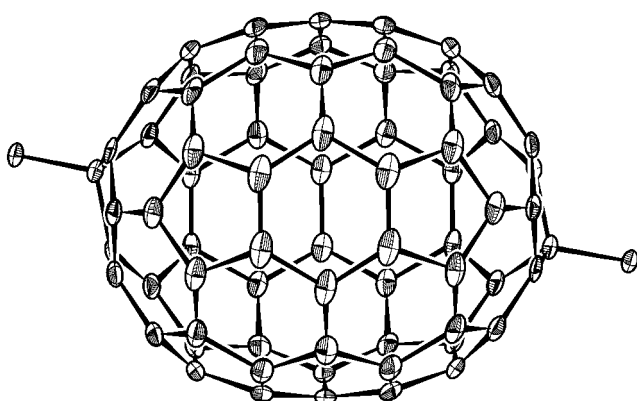


Figure 2. Structure of a C_{70}^{2-} monomeric unit viewed along the non-crystallographic twofold rotation axis (anisotropic displacement ellipsoids drawn at the 70% probability level).

All non-hydrogen atoms of **2**, including the carbon atoms of the fullerene cage, could be refined by using anisotropic displacement parameters without applying any geometrical or non-crystallographic constraints. The rigid-body motion analysis (TLS model)^[14] of the fullerene fragment converges to the reliability factors $R_1=0.073$ and $R_2=0.071$. The mean square libration amplitudes ($\lambda_1=5.22(^{\circ})^2$, $\lambda_2=1.35(^{\circ})^2$,

$\lambda_3=1.14(^{\circ})^2$) point to a librational motion around the axis of the polymer. Since all carbon atoms are placed on a ellipsoidal surface, shortening of the C–C bond lengths due to this libration is within the size of the estimated standard deviations, that is, it is very small.

Within the chains, the angle defined by the centres of mass of three successive fullerene cages is 153.2° . The chains are arranged along [001] as a hexagonal close packing of rods (Figure 4). The smallest separations between two centres of mass are 10.493 Å within one chain, and 10.023 Å between two neighbouring chains. The latter distance corresponds to the van der Waals diameter of C_{70} and points to, at most, van der Waals type intermolecular interactions.

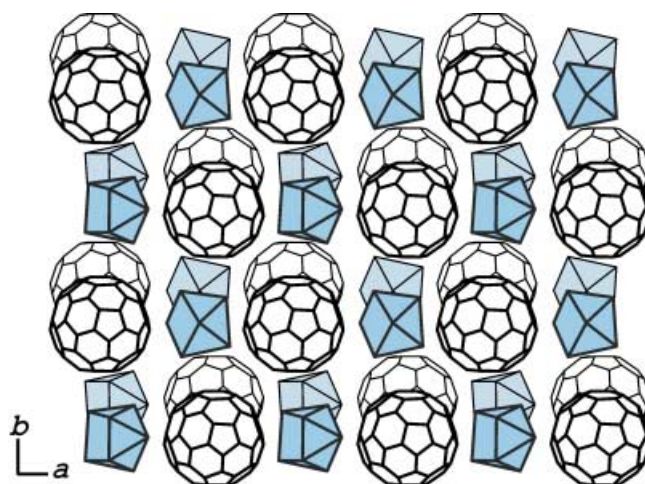


Figure 4. Crystal structure of **2** viewed along the ${}_{\infty}[\text{C}_{70}^{2-}]$ chains.

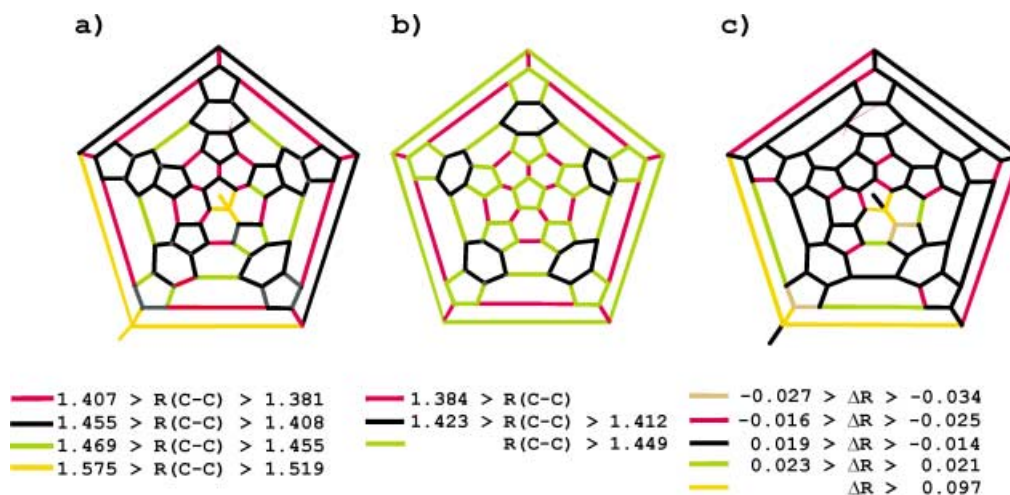


Figure 3. Schlegel diagrams showing the C–C bond lengths in Å. a) ${}_{\infty}[\text{C}_{70}^{2-}]$ (exptl), b) in C_{70} (HF, SV) and c) the structural changes in $[\text{C}_{70}(\text{CH}_3)_2]^{2-}$ relative to C_{70} (HF, SV).

The cationic substructure consists of strontium atoms, coordinated by eight ammonia molecules forming a distorted, dicapped trigonal prism (Figure 5) with Sr–N bond lengths in

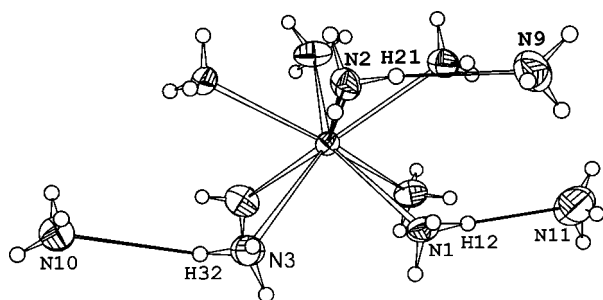


Figure 5. Structure of the cationic unit (anisotropic displacement ellipsoids drawn at the 70% probability level). Strontium atoms are coordinated by eight ammonia molecules forming a distorted, dicapped trigonal prism (Sr–N bond lengths are 2.678(2)–2.827(2) Å). Three of these eight ammonia molecules act as donors to form weak hydrogen bonds to further ammonia molecules of crystallisation.

the range of 2.678(2)–2.827(2) Å. Three of these eight ammonia molecules act as donors to form weak hydrogen bonds to further ammonia molecules of crystallisation (Table 1). The coordination of the alkaline earth metal cation in **2** is different from that in **1**, in which nine ammonia molecules form a tricapped trigonal prism around the barium atoms and seven of them are coordinated to a further ammonia solvent molecule. The higher amount of NH₃ in **1** is in agreement with a higher volume of the unit cell (5315 Å³ in **1** and 4592 Å³ in **2**).

Table 1. Hydrogen bonds in the cationic unit of [Sr(NH₃)₈]C₇₀·3NH₃.

	<i>d</i> (D–H) [Å]	<i>d</i> (H...A) [Å]	<i>d</i> (D...A) [Å]	∠DHA [°]
N1–H12...N11	0.92(4)	2.28(4)	3.204(7)	178(2)
N2–H21...N9	0.90(4)	2.38(5)	3.270(6)	169(2)
N3–H32...N10	0.89(4)	2.654(5)	3.522(7)	164(3)

Hydrogen atoms exhibit the shortest intermolecular distances to the fulleride anions, as has also been observed in another group of well-characterised ammonia-containing fullerides, [M(NH₃)₆]C₆₀·6NH₃ (M = Mn, Co, Ni, Zn, Cd)^[15] and [Ba(NH₃)₇]C₆₀·NH₃.^[16] Thus, an interaction of the N–H dipoles with the electron density of the fulleride surface can be assumed.

The crystallographic data of **2** are given in Table 2. Preliminary investigations of the system Ba/C₇₀/NH₃ show evidence for the existence of a monoclinic phase with *a* = 16.04 Å, *b* = 16.09 Å, *c* = 20.03 Å, β = 123.0°, isostructural to **2**. On the other hand no orthorhombic phase isostructural to **1** has yet been observed in the system Sr/C₇₀/NH₃.

Ab-initio calculations: To investigate the fulleride structure by ab-initio methods, we have modelled the polymeric chain by the monomeric dianions saturated at the bridging carbon atoms by either hydrogen atoms [C₇₀H₂]²⁻ or by methyl groups [C₇₀(CH₃)₂]²⁻ without applying structural constraints in the

Table 2. Crystallographic data for [Sr(NH₃)₈]C₇₀·3NH₃.

crystal size [mm ³]	0.5·0.2·0.1
space group	<i>P</i> 2 ₁ / <i>c</i>
pearson symbol	<i>mP</i> 460
<i>a</i> [Å]	16.345(1)
<i>b</i> [Å]	16.373(1)
<i>c</i> [Å]	20.301(4)
β [°]	122.55(2)
<i>V</i> [Å ³]	4592(2)
<i>Z</i>	4
ρ [g cm ⁻³]	1.614
μ [mm ⁻¹]	0.681
<i>F</i> (000)	2272
<i>T</i> [K]	93
2θ _{max} [°]	44.0
index range	–21 ≤ <i>h</i> ≤ 21 –21 ≤ <i>k</i> ≤ 21 –25 ≤ <i>l</i> ≤ 25
reflections measured	80 457
unique reflections	10 944
parameters/restraints	871/0
absorption correction	numerical
<i>R</i> _{int}	0.057
<i>R</i> ₁	0.038
<i>wR</i> ₂ (all data)	0.097
Δ <i>F</i> _{min} /Δ <i>F</i> _{max} [e Å ⁻³]	0.58/–0.31

calculations. The bond lengths in the fully optimised structures of the two model compounds differ by only 0.001 Å, except for the single bonds to the substituted carbon atom for which the difference is up to 0.004 Å. In the further discussion only the results for [C₇₀(CH₃)₂]²⁻ are considered. To ensure the validity of the theoretical results different methods (Hartree–Fock as well as density functional theory with either local (LDA) or gradient-corrected (GGA) functionals) and various basis sets (minimal basis (STO-3G), split valence basis (SV) and valence triple zeta including polarisation functions (TZVP)) were applied. In Table 3, the respective

Table 3. Deviations (mean value (standard deviation) in Å) of the C–C bond lengths in [C₇₀(CH₃)₂]²⁻ from the experimental values for [C₇₀]²⁻.

Basis	STO-3G	SV	TZVP
HF	0.003 (0.013)	0.002 (0.008)	–0.008 (0.009)
DFT (LDA; S-VWN)	0.014 (0.004)	0.006 (0.005)	–0.007 (0.005)
DFT (GGA; B-LYP)	0.039 (0.005)	0.025 (0.004)	0.012 (0.004)

mean errors and their standard deviations of all C–C bonds in the carbon cage relative to the corresponding experimental values for **2** are given. The bond lengths obtained with the gradient-corrected functional are too large, especially with small basis sets. Concerning the other methods, the mean error is 0.01 Å and smaller. The slightly larger standard deviation of the bond length errors at the Hartree–Fock level is due to an overestimation of the bond alternation. Short C–C bonds are slightly too short and long bonds are too long.

Except for DFT with both the gradient-corrected functional and a small basis set, the large variations of the C–C bond lengths in C₇₀ units in **2** ranging from 1.39 Å to 1.54 Å (Figure 3a) are very well reproduced by the ab-initio calculations, and thus also the structural changes of C₇₀ due to reduction and polymerisation (Figure 3b and c).

The bonds to the bridging carbon atoms connected to the adjacent C_{70} cages in the polymer and to the methyl groups in the model compound are strongly elongated. These bridging atoms can be described as sp^3 -hybridised carbon atoms. Further considerable distortions can be observed only in the vicinity of the sp^3 centers. The six-membered rings forming a phenylene-type belt around the C_{70} cages are nearly unaffected.

The structural features are generally in agreement with the results of the analysis of the electron localisation function (ELF).^[17] The domains of the ELF exhibit a characteristic shape depending on the bonding character in $[C_{70}(CH_3)_2]^{2-}$ (Figure 6). The topological analysis of the ELF and the integration of the electron density within the basins of the resulting ELF attractors^[18] makes it possible to clearly distinguish the various bonding types in the carbon cage. Within the basins of the six-membered rings in the equator of the cage (view 4 in Figure 6), the integrated electron numbers (HF, SV basis set) vary from 2.46 to 3.04. These bonds are chemically similar to aromatic ones. The corresponding number is 2.83 in benzene.^[19]

In the caps of the cage, the bonding is comparable to conjugated hydrocarbons. In the region displayed in view 3 in Figure 6 we obtain 3.29 and 3.38 electrons in the basins of the short bonds (1.38 Å) and 2.34 electrons in the basin of the longer bond (1.45 Å). The related numbers in *trans*-butadiene are 2.17 for the central and 3.56 for the terminal bonds.^[19] In contrast to *trans*-butadiene one only finds one disynaptic attractor in the short C–C bonds, due to the nonplanarity of the system. At a closer look, the bonding situation is far more complicated, especially around atoms with small angular sums ($\sim 345^\circ$) such as the atoms coloured in green (view 2 in Figure 6). At these atoms monosynaptic attractors appear outside the cage whose basins carry up to 0.8 electrons leading to a reduction of the electron numbers in the adjacent bonds.

The basins of bonds including the bridging atoms contain less than two electrons, that is, these are attributed to single bonds (view 1 in Figure 6). The sp^3 character of the bridging atoms leads to monosynaptic attractors with electron numbers of 1.0 at one of the neighbouring atoms (coloured blue in view 1 of Figure 6), although these atoms have a rather large angular sum (351.9°). These atoms seem to be the preferred reaction sites for an additional bond to the neighbouring monomer to form the four-membered rings that are observed in the neutral polymeric C_{70} obtained under pressure.^[3a]

The double negative charge is distributed over the whole cage. The insufficient accuracy and the basis-set dependence of the various population analysis methods does not allow us to definitely assign charges to the single atoms. Only at the “blue atoms” described above, a slight accumulation of negative charge can be observed clearly. A trend to a small negative partial charge on atoms with small angular sums appears to be present but is not significant.

At the HF STO-3G level the monomeric C_{70}^{2-} ion is significantly less stable than our model system for the polymer. Local minima are more than 5 eV higher in energy than those of $[C_{70}H_2]^{2-}$ corrected for the energy of 2H. From these calculations no firm conclusion can be drawn about the relative stability of the different spin states (closed-shell singlet versus triplet), since the energy difference is in the range of a few kJ mol^{-1} and of opposite sign in HF and DFT. Compared to the neutral C_{70} the structure of the dianion is strongly distorted in the six-membered rings in the phenylene-type belt of the cage. In the polymer the gain of energy goes along with the removal of these distortions.

Raman spectra: The Raman spectra of polycrystalline $AC_{70} \cdot nNH_3$ ($A = Ca, Eu, Yb$), **1** and **2** exhibit characteristic bands of C_{70} (Figure 7). Due to symmetry reduction additional resonances appear.

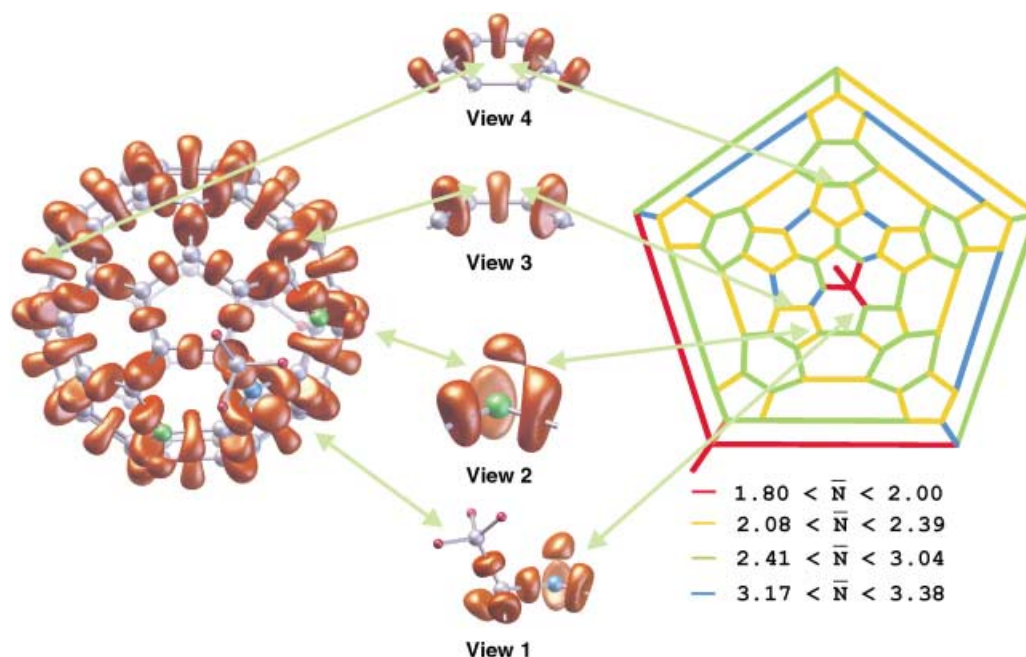


Figure 6. Domains of the electron localisation function (ELF = 0.8) of $[C_{70}(CH_3)_2]^{2-}$ (HF, SV). The diagram on the right side shows the integrated electron densities within the basins of the disynaptic attractors.

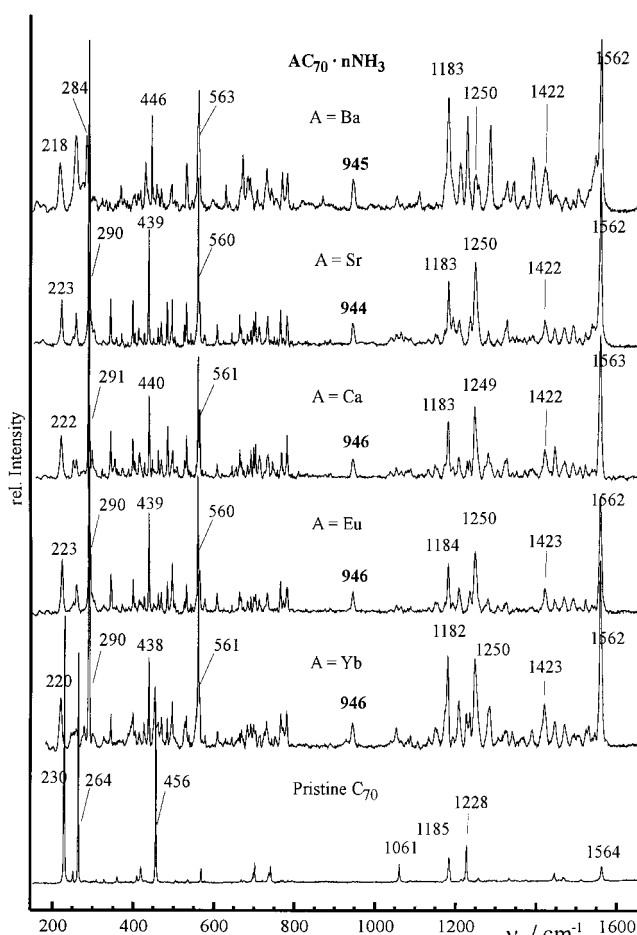


Figure 7. Room-temperature Raman spectra of $AC_{70} \cdot nNH_3$ ($A = Ca, Sr, Ba, Eu, Yb$) and pristine C_{70} .

The most striking feature of the Raman spectra is the appearance of an additional band at $\tilde{\nu} = 945 \text{ cm}^{-1}$, comparable to those observed in the spectra of linked fullerenes.^[1a, 3, 5a, 6, 20] In most cases these are not discussed in detail. To the best of our knowledge, these resonances correspond to skeletal $\nu_{as}(C-C)$ of the sp^3 carbon atoms.

Conclusion

We present a new way to synthesise fulleride compounds of ammonia coordinated divalent alkaline earth and rare earth metals which contain linear polymeric, anionic chains $_{\infty}[C_{70}^{2-}]$. The fulleride substructure is the same for all the cations under investigation as was shown by Raman spectroscopy. The reduced mobility of C_{70} cages in the crystal, caused by the covalent linking, makes it possible to determine precisely the individual positions of the carbon atoms in the cage by single-crystal X-ray structure analysis. This has been shown for the Sr compound. Hartree–Fock and density functional calculations, except those in which a gradient-corrected functional combined with a small basis set is used, reproduce very well the structural features measured experimentally. As confirmed by the analysis of the electron localisation function the structure includes a large variety of

C–C bonding types, ranging from single bonds at the bridging atoms, conjugated double bonds in the caps of the C_{70} cage and bonds in the phenylene-type ring that are comparable to those of aromatic compounds. The stability of this ring, going along with the preservation of its aromaticity, is decisive for the observed reaction behaviour and for the tendency of forming polymeric anions. Chemical reactions at C_{70} happen at specific sites, leading to rather localised distortions of the structure of the cage. Since they cannot be explained considering only symmetry and topology, theoretical investigations implying structural or symmetry constraints should be rated cautiously.

Experimental Section

Stoichiometric amounts of metal (Ca, Sr, Ba, Eu or Yb) and C_{70} were placed in an ampoule ($d = 8 \text{ mm}$), fused onto the base of an oven-dried Schlenk vessel, keeping inert gas conditions. The Schlenk vessel was subsequently evacuated and filled with ammonia by condensation. The reaction mixture was frozen with liquid nitrogen and the glass ampoule was sealed. After three weeks at -33°C , the ampoule was slowly heated to room temperature and then stored for several months. During this period, the solution which was initially blue changed to red-brown. Usually polycrystalline solids were formed, while in one case (Sr) shiny black single crystals were obtained.

Crystal structure determination: An ampoule containing single crystals was refrozen with liquid nitrogen, and opened and thawed under inert gas conditions. Liquid and crystals were transferred into degassed and cooled perfluoropolyether oil (Galden HT230). A crystal suitable for single-crystal X-ray analysis was removed from the oil with a glass capillary attached to a preadjusted goniometer head. The crystal was immediately cooled with liquid nitrogen and placed on the diffractometer.

The data were collected on a STOE IPDS diffractometer at 93 K with $Ag_{K\alpha}$ radiation ($\lambda = 0.56086 \text{ \AA}$). The structure was solved by direct methods (SHELXS-97).^[21] The positions of the carbon and hydrogen atoms were located using difference Fourier maps (SHELXL-97).^[22] All non-hydrogen atoms were refined anisotropically and H atoms isotropically without any constraints.

CCDC-166142 contains the supplementary crystallographic data for this paper. These data can be obtained free of charge via www.ccdc.cam.ac.uk/conts/retrieving.html (or from the Cambridge Crystallographic Data Centre, 12 Union Road, Cambridge CB21EZ, UK; fax: (+44) 1223-336-033; or deposit@ccdc.cam.ac.uk).

Computational studies: Hartree–Fock and DFT calculations were performed with three different basis sets: a minimal basis set (STO-3G^[23]), a split valence basis set (SV^[24]) and a triple valence zeta basis set including polarisation functions (TZVP^[25]). We used either the Gaussian 98 program package^[26] or TURBOMOLE,^[27] the latter especially for the calculations with large basis sets or for RI-DFT.^[28] The DFT calculations were performed in the local density approximation (S-VWN: exchange: Slater $\rho^{4/3}$; correlation: Vosko, Wilk, Nusair,^[29] recommended functional-VWN5 in Gaussian notation) or with a gradient-corrected functional (B-LYP: exchange: Becke;^[30] correlation: Lee, Yang, Parr^[31]). In the structure optimisations with TURBOMOLE the convergence criteria were set to 10^{-8} Hartree for the energy and to 10^{-5} Hartree/Bohr for the norm of the cartesian gradient. At the HF-SV-level the force constant matrix and the vibrational frequencies were computed. No negative eigenvalues were found, indicating the convergence to a local minimum of the energy hypersurface. Based on the HF-SV wavefunction the electron density and the electron localisation function were analysed topologically^[18, 32] with the TopMoD program package.^[33] Besides this, various other population analysis methods were used.

Raman spectroscopy: Raman measurements were performed with a microscope laser Raman system (Jobin-Yvon, LabRAM) with an He-Ne laser (632.8 nm) for excitation. The spectra were recorded with a laser power of 4 mW at a resolution of 4 cm^{-1} and corrected for luminescence

background. The laser was focused on a sample through the glass wall of the pressure ampoule. In all cases the polycrystalline solids, and for the strontium compound the crystals, were studied. Because of technical limitations of the Raman spectrometer it has up to now not been possible to look for low-frequency Raman modes, which are predicted for interstage vibrational modes.

Acknowledgement

This work was supported by the Fond der Chemischen Industrie. Furthermore the authors would like to thank Dr. O. Oeckler for the single crystal X-ray measurements, Dr. H. Vogt for measuring the Raman spectra and Dr. M. Panthöfer for useful discussions.

- [1] a) J. Winter, H. Kuzmany, A. Soldatov, P. Persson, P. Jacobsson, B. Sundqvist, *Phys. Rev. B* **1996**, *54*, 17486; b) C. Stephens, G. Bortel, G. Faigel, M. Tegze, A. Janossy, S. Pekker, G. Oszlanyi, L. Forro, *Nature* **1994**, *370*, 636.
- [2] A. Rao, P. Zhou, K. Wang, G. Hager, *Science* **1993**, *259*, 955.
- [3] a) A. Rao, M. Eklund, J. Hodeau, L. Marques, M. Nunez-Regueiro, *Phys. Rev. B* **1997**, *55*, 4766; b) Y. Iwasa, T. Arima, *Science* **1994**, *264*, 1570.
- [4] G. Wang, K. Komatsu, Y. Murata, M. Shiro, *Nature* **1997**, *387*, 583.
- [5] a) S. Lebedkin, W. Hull, A. Soldatov, B. Renker, M. Kappes, *J. Phys. Chem.* **2000**, *104*, 4101; b) M. Premila, C. Sundar, P. Sahu, A. Bharathi, Y. Hariharan, D. Muthu, A. Sood, *Solid State Commun.* **1997**, *104*, 237.
- [6] A. Soldatov, G. Roth, A. Dzyabchenko, D. Johnels, S. Lebedkin, C. Meingast, B. Sundqvist, M. Haluska, H. Kuzmany, *Science* **2001**, *293*, 680.
- [7] a) A. Hönnerscheid, L. van Wullen, M. Jansen, J. Rahmer, M. Mehring, *J. Chem. Phys.* **2001**, *115*, 7161; b) A. Hönnerscheid, R. Dinnebier, M. Jansen, *Acta Crystallogr. Sect. B*, in press; c) G. Oszlanyi, G. Bortel, G. Faigel, L. Granasy, G. Bendele, P. Stephens, L. Forro, *Phys. Rev. B* **1996**, *54*, 11849.
- [8] A. Hirsch, B. Nuber, *Acc. Chem. Res.* **1999**, *32*, 795.
- [9] G. Bendele, P. Stephens, K. Prassides, K. Vavekis, K. Kordatos, K. Tanigaki, *Phys. Rev. Lett.* **1998**, *80*, 736.
- [10] S. Maradonna, K. Prassides, K. Knudsen, M. Hanfland, M. Kosaka, K. Tanigaki, *Chem. Mater.* **1999**, *11*, 2960.
- [11] G. Oszlanyi, G. Baumgartner, G. Faigel, L. Forro, *Phys. Rev. Lett.* **1997**, *78*, 4438.
- [12] H. Brumm, E. Peters, M. Jansen, *Angew. Chem.* **2001**, *113*, 2117; *Angew. Chem. Int. Ed.* **2001**, *40*, 2069.
- [13] M. Bühl, A. Hirsch, *Chem. Rev.* **2001**, *101*, 1153.
- [14] a) V. Schomaker, K. N. Trueblood, *Acta Crystallogr. Sect. B* **1968**, *24*, 63; b) A. L. Spek, PLATON 2000, A Multipurpose Crystallographic Tool, Utrecht University (The Netherlands), **2000**.
- [15] a) K. Himmel, M. Jansen, *Chem. Commun.* **1998**, 1205; b) K. Himmel, M. Jansen, *Eur. J. Inorg. Chem.* **1998**, 1183; c) H. Brumm, M. Jansen, *Z. Anorg. Allg. Chem.* **2001**, *627*, 1.
- [16] K. Himmel, M. Jansen, *Inorg. Chem.* **1998**, *37*, 3437.
- [17] a) A. D. Becke, K. E. Edgecombe, *J. Chem. Phys.* **1990**, *92*, 5397; b) A. Savin, A. D. Becke, J. Flad, R. Nesper, H. Preuss, H. G. von Schnering, *Angew. Chem.* **1991**, *103*, 421; *Angew. Chem. Int. Ed. Engl.* **1991**, *30*, 409.
- [18] B. Silvi, A. Savin, *Nature* **1994**, *371*, 683.
- [19] A. Savin, B. Silvi, F. Colonna, *Can. J. Chem.* **1996**, *74*, 1088.
- [20] a) G. Adams, J. Page, *Phys. Status Solidi B* **2001**, *226*, 95; b) H. Schober, B. Renker, R. Heid, *Phys. Rev. B* **1999**, *60*, 998; c) V. A. Davydov, L. S. Kashevarova, A. V. Rakhmanina, V. Agafonov, H. Allouchi, R. Ceolin, A. V. Dzyabchenko, V. M. Senyavin, H. Szwarc, *Phys. Rev. B* **1998**, *58*, 14786; d) T. Wagberg, P. Jacobsson, B. Sundqvist, *Phys. Rev. B* **1999**, *60*, 4535; e) J. Arvanitidis, K. P. Meletov, K. Papagelis, A. Soldatov, K. Prassides, G. A. Kourouklis, S. Ves, *Phys. Status Solidi B* **1999**, *215*, 443.
- [21] G. M. Sheldrick, SHELXS-97, Program for Crystal Structure Determination, University of Göttingen (Germany), **1997**.
- [22] G. M. Sheldrick, SHELXL-97, Program for the Refinement of Structures, G. M. Sheldrick, University of Göttingen (Germany), **1997**.
- [23] W. J. Hehre, R. F. Stewart, J. A. Pople, *J. Chem. Phys.* **1969**, *51*, 2657.
- [24] A. Schäfer, H. Horn, R. Ahlrichs, *J. Chem. Phys.* **1992**, *97*, 2571.
- [25] A. Schäfer, C. Huber, R. Ahlrichs, *J. Chem. Phys.* **1994**, *100*, 5829.
- [26] Gaussian 98 (Revision A.7), M. J. Frisch, G. W. Trucks, H. B. Schlegel, G. E. Scuseria, M. A. Robb, J. R. Cheeseman, V. G. Zakrzewski, J. A. Montgomery, R. E. Stratmann, J. C. Burant, S. Dapprich, J. M. Millam, A. D. Daniels, K. N. Kudin, M. C. Strain, O. Farkas, J. Tomasi, V. Barone, M. Cossi, R. Cammi, B. Mennucci, C. Pomelli, C. Adamo, S. Clifford, J. Ochterski, G. A. Petersson, P. Y. Ayala, Q. Cui, K. Morokuma, D. K. Malick, A. D. Rabuck, K. Raghavachari, J. B. Foresman, J. Cioslowski, J. V. Ortiz, B. B. Stefanov, G. Liu, A. Liashenko, P. Piskorz, I. Komaromi, R. Gomperts, R. L. Martin, D. J. Fox, T. Keith, M. A. Al-Laham, C. Y. Peng, A. Nanayakkara, C. Gonzalez, M. Challacombe, P. M. W. Gill, B. G. Johnson, W. Chen, M. W. Wong, J. L. Andres, M. Head-Gordon, E. S. Replogle, J. A. Pople, Gaussian Inc., Pittsburgh PA (USA), **1998**.
- [27] R. Ahlrichs, Turbomole Version 5.3, Quantum Chemistry Group, University of Karlsruhe (Germany), **2000**.
- [28] K. Eichkorn, O. Treutler, H. Öhm, M. Häser, R. Ahlrichs, *Chem. Phys. Lett.* **1995**, *242*, 652.
- [29] S. H. Vosko, L. Wilk, M. Nusair, *Can. J. Phys.* **1980**, *58*, 1200.
- [30] A. D. Becke, *Phys. Rev. A* **1988**, *38*, 3098.
- [31] C. Lee, W. Yang, R. G. Parr, *Phys. Rev. B* **1988**, *37*, 785.
- [32] R. F. W. Bader, *Atoms in Molecules; A Quantum Theory*, **1990**, Oxford University Press, Oxford (UK).
- [33] S. Noury, X. Krokidis, F. Fuster, B. Silvi, ToPMoD, Université Pierre et Marie Curie, Paris (France), **1997**.

Received: January 28, 2002 [F 3830]